doi:10.1006/jmbi.2001.4958 available online at http://www.idealibrary.com on IDEAL® *J. Mol. Biol.* (2001) **312**, 637–647

JMB

High Affinity Cooperative DNA Binding by the Yeast Mlh1-Pms1 Heterodimer

Mark C. Hall[1], Hong Wang[2], Dorothy A. Erie[2] and Thomas A. Kunkel[1]*

[1]*Laboratories of Molecular Genetics and Structural Biology, NIEHS, RTP, NC 27709, USA*

[2]*Department of Chemistry University of North Carolina Chapel Hill, NC 27599, USA*

**Corresponding author*

We demonstrate here that the *Saccharomyces cerevisiae* Mlh1-Pms1 heterodimer required for DNA mismatch repair and other cellular processes is a DNA binding protein. Binding was evaluated using a variety of single and double-stranded DNA molecules. Mlh1-Pms1 bound short substrates with low affinity and showed a slight preference for single-stranded DNA. In contrast, Mlh1-Pms1 exhibited a much higher affinity for long DNA molecules, suggesting that binding is cooperative. High affinity binding required a duplex DNA length greater than 241 base-pairs. The rate of association with DNA was rapid and dissociation of protein-DNA complexes following extensive dilution was very slow. However, in competition experiments, we observed a rapid active transfer of Mlh1-Pms1 from labeled to unlabeled DNA. Binding was non-sequence specific and highly sensitive to salt type and concentration, suggesting that Mlh1-Pms1 primarily interacts with the DNA backbone *via* ionic contacts. Cooperative binding was observed visually by atomic force microscopy as long, continuous tracts of Mlh1-Pms1 protein bound to duplex DNA. These images also showed that Mlh1-Pms1 simultaneously interacts with two different regions of duplex DNA. Taken together, the atomic force microscope images and DNA binding assays provide strong evidence that Mlh1-Pms1 binds duplex DNA with positive cooperativity and that there is more than one DNA binding site on the heterodimer. These DNA binding properties of Mlh1-Pms1 may be relevant to its participation in DNA mismatch repair, recombination and cellular responses to DNA damage.

Keywords: mismatch repair; Mlh1; Pms1; MutL homologs; DNA binding; recombination

Introduction

The DNA mismatch repair systems of prokaryotes and eukaryotes serve a vital function in maintaining genomic stability by correcting replication errors that escape polymerase proofreading and by discouraging recombination between homeologous DNA sequences (for recent reviews see Buermeyer *et al*.; Kolodner & Marsischky; Harfe & Jinks-Robertson).[1–3] The *Escherichia coli* DNA mismatch repair pathway is the best characterized and has been fully reconstituted *in vitro*.[4] The dimeric MutS protein initiates repair by recognizing a DNA mismatch.[5] MutL binds to a MutS-mismatch complex[6] and links it to the MutH-catalyzed incision of the newly replicated DNA strand at a nearby hemimethylated 5′-GATC-3′ sequence.[7–9] The incision serves as an entry point for UvrD (DNA helicase II)[10] to displace the error-containing DNA strand, which is degraded by one of several exonucleases. The resulting gap is filled in by DNA polymerase III holoenzyme and sealed by DNA ligase.[4]

Two of the *E. coli* mismatch repair proteins, MutS and MutL, have homologs in eukaryotic mismatch repair systems, suggesting that early steps in the pathway are evolutionarily conserved. Homologs have not been found for many of the downstream components of the *E. coli* pathway, indicating that following mismatch recognition, there may be substantial divergence in the repair mechanism. While much attention has been focused on studying the MutS homologs and their role in initiating mismatch repair through mismatch recognition, many details of the role of the MutL homologs are still unknown. In the past few years, substantial progress has been made in char-

Abbreviations used: ss, single-stranded; ds, double-stranded; AFM, atomic force microscopy.

E-mail address of the corresponding author: kunkel@niehs.nih.gov

0022-2836/01/040637–11 $35.00/0

acterizing the *E. coli* MutL protein. MutL interacts with three other enzymes in the pathway, MutS,[6] MutH[8,9] and UvrD,[11] and it stimulates the activity of each of these proteins.[8,9,12,13] Thus, MutL acts as a central coordinator of the serial reactions that occur during the correction of a DNA mismatch. MutL possesses a weak ATPase activity[8] that is essential for mismatch repair.[14] In addition, MutL was shown to be a DNA binding protein with affinity for both ssDNA and dsDNA.[8,15–17] In most of those studies, DNA binding appeared to be relatively weak. Possibly for this reason, DNA binding by MutL has not yet been investigated extensively. In fact, most current models for DNA mismatch repair do not invoke direct MutL interaction with the DNA substrate.

It has become clear in recent years that eukaryotic mismatch repair proteins participate in a variety of other DNA transactions. These include transcription-coupled nucleotide excision repair, DNA damage surveillance, cell cycle checkpoint control and apoptosis, meiotic chromosome pairing and crossing-over, and possibly somatic hypermutation of immunoglobulin genes (reviewed by Buermeyer *et al.*[1]). Of particular interest, the eukaryotic MutL homologs MLH1 and PMS2 are the only mismatch repair proteins currently known to play a central role in meiosis.[1] Mice lacking MLH1 or PMS2 show defects in meiosis that suggest a role in chromosome synapsis and meiotic crossing over.[18–20] Similarly, disruption of the yeast *MLH1* gene results in defective meiotic recombination.[21] The widespread involvement of these MutL homologs in DNA metabolic processes raises two interesting questions. Do the heterodimeric eukaryotic MutL homologs bind to DNA? Do all the biological roles of the eukaryotic MutL homologs involve a common set of biochemical properties or are certain properties (e.g. DNA binding) specialized for individual applications?

Here, we demonstrate that the *Saccharomyces cerevisiae* Mlh1-Pms1 heterodimer does indeed bind to DNA. We then report several novel features of this DNA binding activity that have important implications for the many biological functions of Mlh1-Pms1.

Results

Mlh1-Pms1 binds to DNA in a highly salt-sensitive manner

The yeast Mlh1-Pms1 heterodimer was purified to apparent homogeneity as described.[22] We used a nitrocellulose filter binding assay to determine if Mlh1-Pms1 binds to ^{3}H-labeled plasmid (pGBT9) DNA. Binding was observed (Figure 1), and was found to vary as a function of NaCl concentration, both in the presence and absence of 4 mM $MgCl_2$. In the presence of $MgCl_2$, the stability of the protein-DNA complex was greatly reduced compared to the stability in the absence of $MgCl_2$ (Figure 1). The lower stability in the presence of $MgCl_2$ may result from competition between Mg^{2+} and the protein for DNA binding sites, as observed and characterized previously for non-specific protein-DNA interactions.[23] The binding of Mlh1-Pms1 to dsDNA was very sensitive to the concentration of NaCl, as indicated by the steep slopes of the linear portions of the plots in Figure 1. The sensitivity to NaCl (i.e. the slope of the plots) was essentially identical in the presence and absence of $MgCl_2$. The stability of dsDNA-protein complexes was also measured as a function of increasing sodium acetate concentration in the presence of 4 mM magnesium acetate (Figure 1). A much greater concentration of sodium acetate was required to destabilize the (Mlh1-Pms1)-DNA complex compared to NaCl. Acetate ions are expected to bind more weakly to proteins than Cl^- ions based on the Hofmeister series. Therefore, the requirement for a higher concentration of acetate to destabilize the protein-DNA complexes suggests that anion displacement from Mlh1-Pms1 is an important factor in DNA binding. The sensitivity of Mlh1-Pms1 DNA binding to salt concentration, anion type, and the presence of Mg^{2+} is consistent with a non-

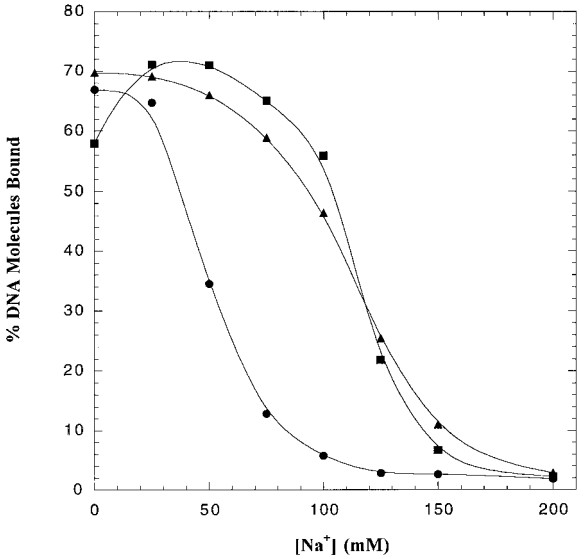

Figure 1. DNA binding by Mlh1-Pms1 is highly sensitive to salt. Nitrocellulose filter binding assays were performed as described in Materials and Methods. Binding was measured as a function of Na^+ concentration using 5 μM [^{3}H]pGBT9 supercoiled DNA (nucleotide concentration) and 90 nM Mlh1-Pms1 (heterodimer concentration). Salt titrations were performed with NaCl in the presence (●) or absence (■) of 4 mM $MgCl_2$ or with sodium acetate in the presence of 4 mM magnesium acetate (▲). All reactions were diluted and filters washed with binding buffer containing the corresponding salt concentration. Data points represent the average of three individual experiments. Kaleidagraph (Synergy Software, Reading, PA) was used to apply a smooth curve fitting algorithm to the data sets to generate the continuous lines.

sequence specific interaction mediated primarily through ionic contacts with the sugar phosphate backbone.

Mlh1-Pms1 dissociates rapidly from labeled DNA only in the presence of unlabeled competitor DNA

To investigate the stability of the (Mlh1-Pms1)-DNA complex, we measured DNA binding as a function of time after 50-fold dilution of the reaction prior to application to filters (Figure 2). For both circular plasmid DNA (pGBT9) and a 153 bp linear dsDNA, protein-DNA complexes did not dissociate for at least four minutes after dilution. For experiments using plasmid DNA, the 50-fold dilution resulted in a final protein concentration of 3.7 nM, a concentration that yields very little binding when added initially to the labeled DNA (see Figure 3). Thus, the binding observed four minutes after dilution cannot be explained by dissociation-reassociation. Note also that the experiment with the 153 bp linear dsDNA substrate (Figure 2, inset) was performed at a low binding density (~12 % of DNA molecules bound), demonstrating that individual protein-DNA interactions are stable during this time. A similar lack of detectable dissociation was observed when M13mp2 ssDNA and short ssDNA oligonucleotides were used (not shown). This slow rate of dissociation following dilution demonstrates that filter binding is a valid approach for measuring Mlh1-Pms1 binding to DNA and that differences observed with long *versus* short DNA substrates (see below) are not due to dissociation.

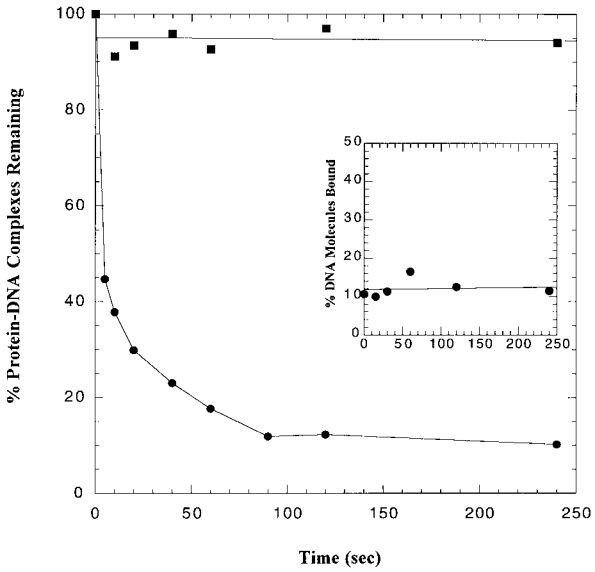

Figure 2. Mlh1-Pms1 dissociates rapidly from labeled DNA only in the presence of unlabeled competitor DNA. Binding reactions were performed as described in Materials and Methods using 5 μM [^{3}H]pGBT9 supercoiled DNA (nucleotide concentration) and 183 nM Mlh1-Pms1 (heterodimer concentration). After a ten minute incubation, 168-fold excess unlabeled pGBT9 was added and the reaction incubated for the indicated amount of time (●) or reactions were diluted with a 50-fold excess of binding buffer and incubated for the indicated amount of time (■) prior to application to the filter. Results were normalized to the fraction of protein-bound DNA in the absence of competitor DNA (●), or without further incubation after dilution (■), which was set at 100 %. Data represent the average of three (■) or four (●) independent trials. Inset A 250 nM ^{32}P-labeled 153 bp linear dsDNA (nucleotide concentration) was used in binding reactions with 548 nM Mlh1-Pms1 (heterodimer). After ten minutes, reactions were diluted with 50-fold binding buffer and incubated for the indicated amount of time prior to application to the filter. In this case, the actual fraction of protein-bound DNA molecules was plotted. Horizontal lines in the main graph and inset are linear regressions generated by Kaleidagraph. The smooth line connecting data points (●) was drawn by Kaleidagraph.

In contrast to the slow dissociation from DNA following a 50-fold dilution, Mlh1-Pms1 dissociated very rapidly from [^{3}H]pGBT9 in the presence of an excess of unlabeled pGBT9 (Figure 2). More than half of the initial complexes were completely dissociated in less than five seconds. As the concentration of competitor DNA was increased, the rate of dissociation increased (data not shown). This suggests that, despite its slow rate of passive dissociation from DNA, Mlh1-Pms1 can actively dissociate by a rapid transfer to another DNA strand. The 10 % residual binding after four minutes is observed even when competitor DNA is added prior to protein and therefore most likely does not represent a distinct set of long-lived complexes.

Apparent binding affinity is dramatically higher on long DNA substrates

Previous studies with the *E. coli* MutL protein[8,16] and circumstantial observations with Mlh1-Pms1[24,25] suggest that MutL homologs bind to short oligonucleotide DNA substrates with relatively low affinity. To determine if Mlh1-Pms1 has higher binding affinity for specific DNA substrates or structures, filter binding assays were performed with a variety of ss and dsDNA molecules (Figure 3). All DNA molecules consisting of relatively short ss (Figure 3(a)) and ds (Figure 3(b)) DNA oligonucleotides were bound with low affinity. This collection included DNA substrates that mimic recombination intermediates, such as a Holliday junction (Figure 3(b) (▼)) and a Y-junction (not shown), as well as dsDNA oligonucleotides with 5′ or 3′ ssDNA extensions (not shown).

In contrast to short DNA substrates, the apparent binding affinity of Mlh1-Pms1 for long ssDNA and dsDNA molecules was much higher (Figure 3). Both M13 ssDNA and duplex plasmid DNA (pGBT9) yielded high affinity binding curves compared to the short substrates. Higher affinity was not due to differences in the DNA concentrations used for long and short substrates because control

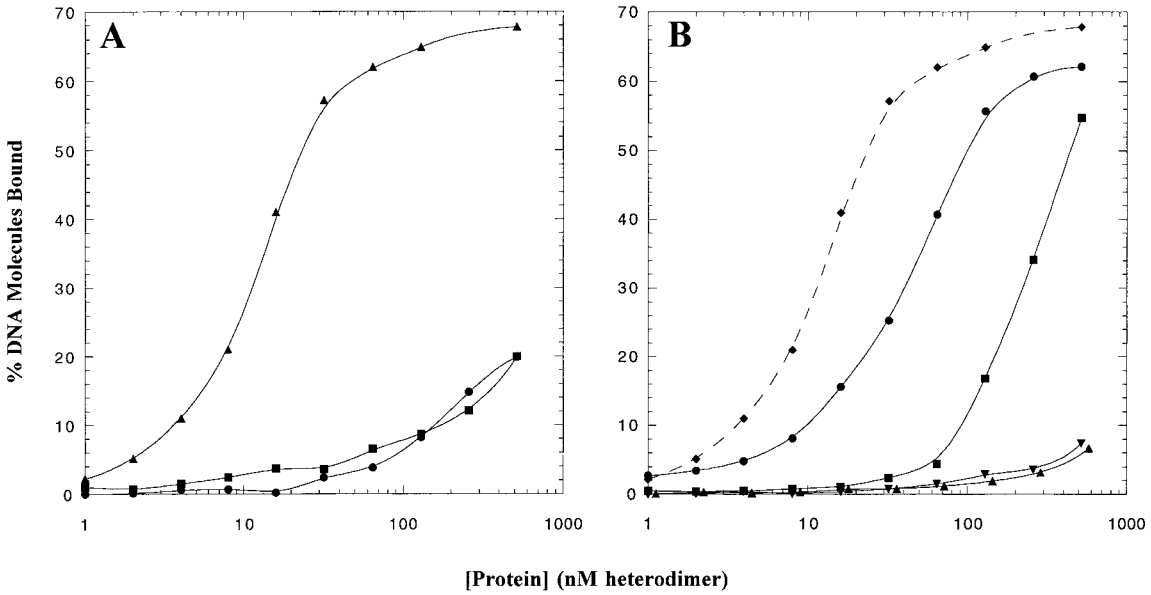

Figure 3. Binding of Mlh1-Pms1 to a variety of DNA substrates. Filter binding assays were performed as a function of protein concentration as described in Materials and Methods. (a) [^{3}H]M13mp2 circular ssDNA (▲) was 5 μM, [^{32}P]poly(dA) (●) was 5 μM, and [^{32}P]100mer ssDNA oligonucleotide (■) was 90 nM. (b) [^{3}H]pGBT9 supercoiled DNA (●) and [^{3}H]pGBT9 linear DNA (■) were 5 μM, [^{32}P]153 bp dsDNA substrate (▲) was 250 nM and the Holliday junction substrate (▼) was 100 nM. [^{3}H]M13mp2 circular ssDNA (◆, broken line) from (a) was replotted in (b) for direct comparison to the dsDNA substrates. All substrates are expressed as DNA nucleotide concentration. Data represent the average of three or four individual trials and smooth lines connecting data points were drawn with Kaleidagraph.

experiments with several different substrates demonstrated convincingly that binding was independent of DNA concentration under our reaction conditions. One explanation for the higher binding affinity of Mlh1-Pms1 for long DNA substrates is positive cooperativity. Interestingly, single-stranded poly(dA) of nearly the same length as the M13 ssDNA was not a high affinity substrate for Mlh1-Pms1 binding (Figure 3). Similar low affinity binding was observed using poly(dT) (not shown). These long synthetic homopolymeric substrates do not have the same potential to form secondary structures as M13 ssDNA, implying that high affinity binding to M13 ssDNA reflects Mlh1-Pms1 interactions with dsDNA regions.

A hierarchy of apparent binding affinities for long DNA substrates

Under identical reaction conditions, supercoiled plasmid DNA was bound with significantly and reproducibly higher apparent affinity than the same plasmid DNA linearized by a restriction endonuclease (Figure 3(b), compare ● to ■). This effect was not related to the superhelicity of the closed circular plasmid DNA, because a similar difference was observed between linear and nicked circular plasmid DNA (data not shown). Furthermore, M13 ssDNA was bound with consistently higher apparent affinity than the supercoiled plasmid DNA. This effect was unrelated to the difference in length between M13 ssDNA and pGBT9 because M13 RFI dsDNA and pGBT9 yielded identical binding curves (data not shown). It is also worth noting that the affinity of Mlh1-Pms1 for linear pGBT9 was still much higher than the affinity for short dsDNA molecules (Figure 3(b)), and that there was no difference in affinity for linear or circular M13 ssDNA (data not shown). The implications of these observations are discussed below.

Effect of linear dsDNA length on apparent binding affinity

We measured the interaction of Mlh1-Pms1 with linear dsDNA as a function of the DNA chain length to determine the length of dsDNA required to obtain high affinity binding (Figure 4). Restriction fragments of pGBT9 were generated and labeled with ^{32}P in identical fashion. A single concentration of Mlh1-Pms1 was used that results in less than half-maximal binding on the longest DNA substrates, and all DNA substrates were present at an identical nucleotide concentration. The results reveal a sharp increase in binding as the DNA length increased from 241 bp to 513 bp. As the length continued to increase, binding remained essentially constant. The amount of protein-DNA complex formed with the longer substrates present here at 250 nM (30 to 40 % in Figure 4) is similar to the 30 % binding observed when a 20-fold higher concentration of long, linear duplex is used (Figure 3). This confirms the control experiments mentioned above and indicates that the higher

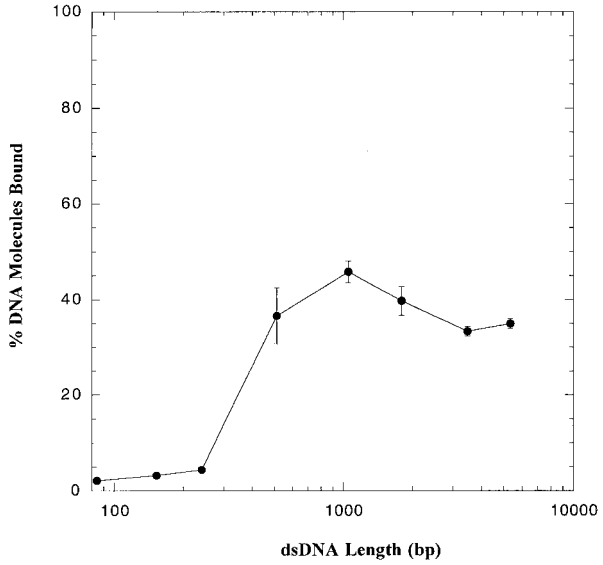

Figure 4. Effect of dsDNA length on binding by Mlh1-Pms1. Filter binding assays were performed as described in Materials and Methods. All [^{32}P]DNA substrates were present in reactions at 250 nM (nucleotide concentration). The concentration of Mlh1-Pms1 in all reactions was 180 nM (heterodimer). Each data point represents the average of four independent experiments and error bars are standard deviations.

DNA binding affinity depends on chain length, not DNA concentration. Therefore, these results are again consistent with a cooperative binding mechanism for Mlh1-Pms1 in which a DNA chain length of greater than 241 bp is required to achieve the cooperative effect.

Figure 4 and the dissociation experiments presented in Figure 2 also suggest that translocation or sliding of Mlh1-Pms1 off DNA ends was not responsible for the difference in apparent affinities between short and long DNA molecules, as shown in Figure 3. It has been suggested that the human Msh2-Msh6 heterodimer, a mismatched DNA recognition protein, forms a topologically constrained ring around DNA capable of sliding or translocating, and that requires a free DNA end to dissociate.[26] Crystal structures of bacterial MutS proteins are consistent with this idea.[27,28] A similar concept of DNA binding *via* formation of a topologically constrained ring around DNA also has been proposed for the *E. coli* MutL protein, based on the crystal structure of an N-terminal 40 kDa fragment.[16] However, if dissociation from free ends were responsible for the observations in Figure 3, then we would not expect to see such a sharp transition from low to high affinity binding as a function of DNA length in Figure 4, and we would expect to see more rapid dissociation of Mlh1-Pms1 from the short 153 bp dsDNA molecule compared to circular dsDNA lacking ends (Figure 2). Therefore, it is unlikely that the presence or absence of DNA ends is a significant factor in the interaction between Mlh1-Pms1 and DNA.

Cooperative binding observed visually using atomic force microscopy

Atomic force microscopy (AFM) was used to directly visualize Mlh1-Pms1 bound to dsDNA. A 1.8 kb plasmid (pMH10; Figure 5) and either circular or linear M13 dsDNA (Figure 6) were deposited onto mica in the presence and absence of Mlh1-Pms1 in the same buffer used for the filter binding assays. In the absence of Mlh1-Pms1 (Figures 5(a) and 6(a)), the DNA molecules showed no high features and appeared very similar to previously published images of circular dsDNA.[29] In the presence of Mlh1-Pms1, the appearance of the DNA molecules was drastically altered by the bound protein (Figure 5(b)-(d) and Figure 6(b) and (c)). Inspection of a large number of such images revealed that the interaction between Mlh1-Pms1 and DNA usually occurred as long, continuous tracts of protein coating the DNA (e.g. see Figures 5(c) and 6(c) and (d)). Singly bound protein molecules were observed at a much lower frequency than those found in tracts. These observations indicate cooperative DNA binding by Mlh1-Pms1.

In the majority of the images of continuous tracts of bound protein, two separate dsDNA regions appeared to be in contact with the protein tracts (Figures 5(b)-(d) and 6(b)-(d)). While there were some long stretches of bound protein associated with only one dsDNA region (Figure 6(c), blue arrow), long, cooperatively bound tracts of protein were observed more often associated with two dsDNA regions (e.g. see Figure 6(c), red arrow). We also observed long tracts of Mlh1-Pms1 bound simultaneously to two separate linear M13 dsDNA molecules (Figure 6(d)) although the occurrence was much less frequent than with the circular dsDNA. This result is consistent with the lower affinity of Mlh1-Pms1 for linear *versus* circular dsDNA observed in filter binding assays (see Figure 3). The AFM results suggest that the Mlh1-Pms1 heterodimer contains more than one DNA binding site and that binding of two duplex DNA strands by Mlh1-Pms1 promotes the formation of long tracts of cooperatively bound protein (see Discussion).

A statistical analysis of the heights of the DNA and DNA-protein complexes observed in the AFM images was performed to confirm that the structures we interpret as two dsDNA regions coated by Mlh1-Pms1 do contain protein and are not simply two interwound dsDNA regions. The height of the DNA alone *versus* the DNA-protein complexes provides a quantitative comparison of the different structures.[30,31] In the absence of protein, the average height of dsDNA was 0.44(±0.08) nm, consistent with a previous study.[32] At intersections where two dsDNA regions cross over each other (e.g. Figure 6(a), arrow), the average height was 0.67(±0.06) nm. In the presence of

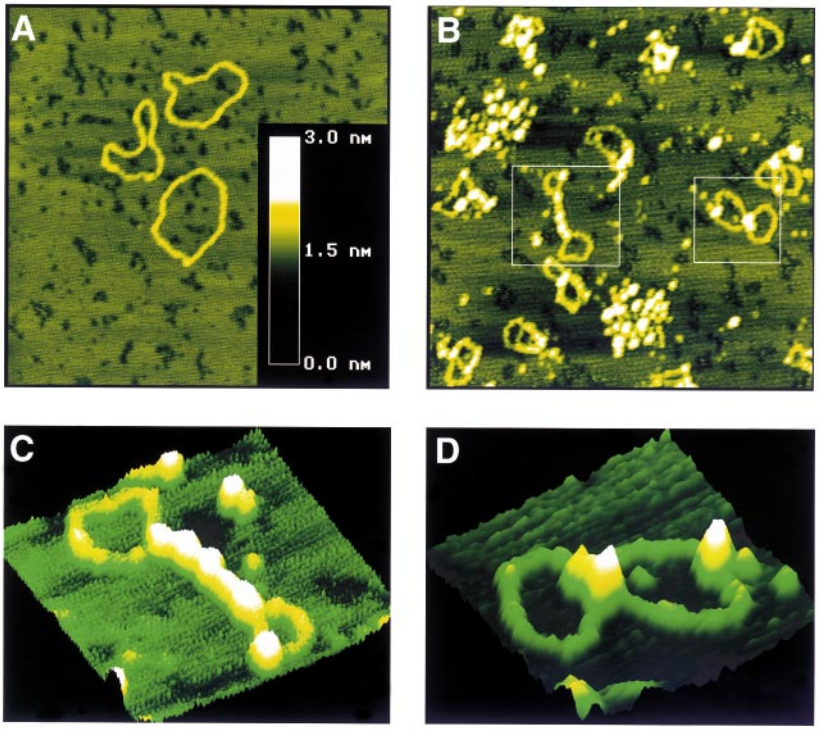

Figure 5. Atomic force microscopy images of Mlh1-Pms1 binding to a 1.8 kb circular dsDNA. AFM images were obtained as described in Materials and Methods. (a) Representative top view of pMH10 DNA alone. The DNA concentration was 15 μM (nucleotide) and the scan size was 900 nm. The color bar (height) representing 0-3.0 nm above the mica surface applies to (a) and (b). (b) Representative top view of 15 μM pMH10 in the presence of 35 nM Mlh1-Pms1. The scan size was 900 nm. (c) and (d) Zoom surface plots of the boxed regions from (b). The plane of the mica was inclined 40° to show the topography of the surface.

Mlh1-Pms1, structures presumably containing protein tracts associated with two dsDNA regions had an average height of 1.42(±0.24) nm. This latter value is too large to be accounted for by two interwound dsDNA regions and we conclude that they are coated with Mlh1-Pms1.

Discussion

This study provides the first direct evidence that a eukaryotic MutL protein complex binds to DNA. Nitrocellulose filter binding and AFM experiments demonstrated that yeast Mlh1-Pms1 binds to both ssDNA and dsDNA in a non-sequence specific manner. In filter binding assays, the affinity of Mlh1-Pms1 for short DNA molecules was low with a slight preference for ssDNA over dsDNA. This result is consistent with previous work on *E. coli* MutL.[16] Surprisingly, the affinity of Mlh1-Pms1 for long DNA molecules was much greater than for short DNA. The data indicate that this increase in affinity on long DNA molecules is a result of strong positive cooperativity, a property not previously reported for any MMR protein. AFM images of protein tracts on dsDNA provide visual confirmation of cooperative binding.

In addition to demonstrating cooperative binding, the AFM images also suggest that the Mlh1-Pms1 heterodimer contains more than one DNA binding site. Moreover, because the majority of protein tracts observed by AFM were associated with two duplex DNA regions, the concomitant occupation of two DNA binding sites on Mlh1-Pms1 may promote the cooperative binding. Several observations from the filter binding experiments provide additional support that the high affinity binding of Mlh1-Pms1 involves multiple dsDNA binding sites in addition to cooperativity. First, the heterodimer binds with higher affinity to circular duplex DNA, whether it is supercoiled or relaxed, than to linear duplex DNA (Figure 3). Circular DNA molecules are more likely than linear molecules to contain two dsDNA regions adjacent to or crossing over each other, thus presenting better opportunities for the binding of Mlh1-Pms1 to both strands and consequent nucleation of a tract of cooperatively bound protein. Second, high affinity binding is only seen when the linear duplex is at least 513 base-pairs (Figure 4). If one assumes that the geometry of the DNA binding sites on Mlh1-Pms1 precludes their occupying adjacent sites on a DNA molecule, then a short, relatively inflexible linear duplex might permit interaction with only a single DNA binding site. Only when the linear duplex DNA molecule is long (i.e. 513 base-pairs), and therefore sufficiently flexible to fold back on itself, will an opportunity exist for a second DNA binding site on Mlh1-Pms1 to be engaged. Although separate DNA molecules in solution would also be available for interaction with the second binding site, intramolecular events should be more favorable. It is also possible that a minimum length of DNA (>241 bp) is required to establish a stable tract of cooperatively bound Mlh1-Pms1 and that this contributes to the DNA length dependence. Third, Mlh1-Pms1 binds with higher affinity to long M13 ssDNA than to long synthetic homopolymeric ssDNA. M13 ssDNA, but not homopolymeric ssDNA, forms a complex array of secondary structures in solution,[29] providing

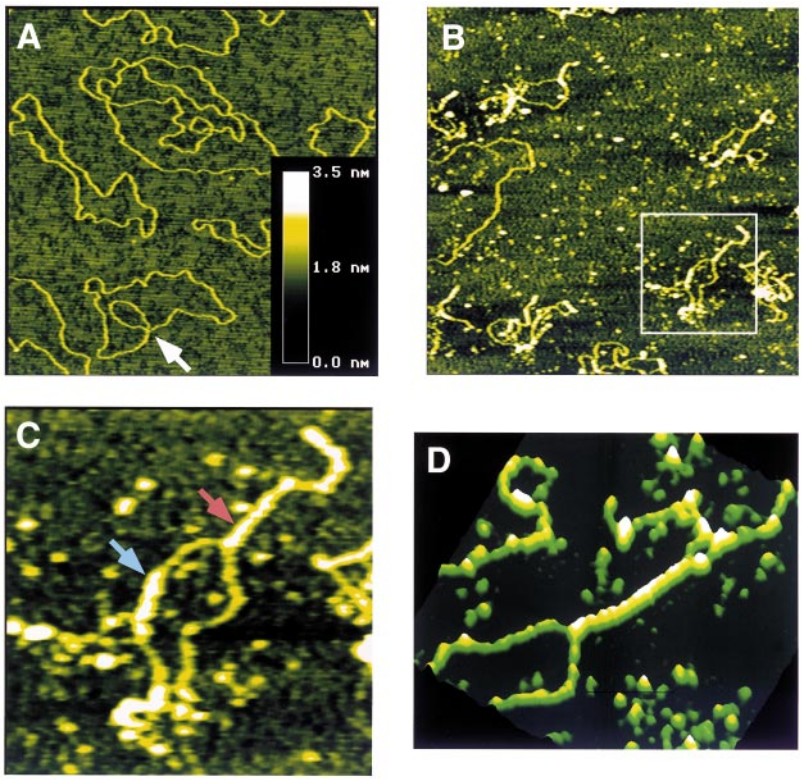

Figure 6. Atomic force microscopy images of Mlh1-Pms1 binding to M13mp2 dsDNA. AFM images were obtained as described in Materials and Methods. (a) Representative top view image of M13mp2 RFI DNA alone. The DNA concentration was 8.7 μM (nucleotide) and the scan size was 1500 nm. The color bar (height) representing 0-3.5 nm above the mica surface applies to (a), (b) and (c). The white arrow points to two dsDNA regions crossing over each other. (b) Representative top view image of 8.7 μM M13 RFI DNA in the presence of 35 nM Mlh1-Pms1. The scan size was 1500 nm. (c) Zoom view of the boxed region from (b). The light blue arrow indicates a tract of cooperatively bound Mlh1-Pms1 associated with a single dsDNA region. The red arrow indicates a tract of cooperatively bound Mlh1-Pms1 associated with two dsDNA regions of a single M13 molecule. (d) Surface plot showing two linear M13 dsDNA molecules held together by a tract of bound Mlh1-Pms1. The DNA concentration was 8.7 μM (nucleotide) and Mlh1-Pms1 was present at 35 nM. The image is an enlargement from an original scan size of 1800 nm. The plane of the mica was inclined 60° to show the topography of the surface.

many opportunities for Mlh1-Pms1 to bind two non-adjacent duplex DNA regions. Furthermore, circular and linear ssDNA would adopt essentially the same configuration in solution, providing an explanation for the observation that circular and linear ssDNA are bound by Mlh1-Pms1 with similar affinity, unlike the situation with circular and linear dsDNA. Finally, two binding sites are consistent with the observation that addition of unlabeled competitor DNA to binding reactions containing stable protein-DNA complexes leads to very rapid dissociation of protein from the labeled DNA (Figure 2). Given the slow rate of passive dissociation of complexes after dilution, this rapid ''switching'' of protein from labeled to unlabeled DNA most likely involves an intermediate in which the protein interacts simultaneously with two DNA molecules.[33]

The concept of more than one DNA binding site in the Mlh1-Pms1 heterodimer differs from a model proposed for DNA binding by homodimeric *E. coli* MutL.[16] Based on structural information, it was suggested that MutL binds ssDNA in a saddle-shaped groove created by the dimerization of MutL N-terminal domains. However, that groove is too small to accommodate duplex DNA. It was further predicted that the C-terminal residues of intact MutL might contribute to formation of a dimeric protein structure that encircles the DNA molecule, thus implying a single DNA binding site within a central hole in the protein. Our results for binding of Mlh1-Pms1 to long duplex DNA imply that alternatives to this model exist for the eukaryotic heterodimer. Nonetheless, the extensive homology and conservation of function implies that similarities may exist in certain DNA binding properties of bacterial MutL and the eukaryotic MutL homologs. For example, Mlh1-Pms1 binding to DNA is highly sensitive to salt concentration and anion type (Figure 1), suggesting interactions of positively charged amino acid side-chains with the DNA backbone. Consistent with this observation, an Arg to Glu mutation has been shown to strongly decrease binding of MutL to DNA.[16] That arginine in MutL is not conserved in Mlh1 or Pms1 and the region of *E. coli* MutL predicted to bind DNA[16] is not highly conserved among MutL homologs at the primary sequence level. However, model building by Ban *et al.*[16] suggests that a positive potential is conserved in the corresponding region of human MLH1-PMS2. We are currently attempting to map the location of DNA binding sites in Mlh1-Pms1 for functional analysis. Similar efforts to identify the sites responsible for cooperative protein-protein interactions also should be informative regarding Mlh1-Pms1 functions.

Current models for DNA mismatch repair[2,3,34] have not invoked a direct interaction of MutL homologs with DNA. Our results indicate that these models may now need revision given the

ability of Mlh1-Pms1 to bind with high affinity to long dsDNA. There is already some evidence that DNA binding by MutL plays a role in mismatch repair in *E. coli*. The interaction of MutL with DNA is important for its ability to stimulate DNA helicase II,[17] the helicase involved in the excision step of the mismatch repair pathway. Furthermore, DNA enhances the ATPase activity of MutL,[16] which is required for mismatch repair[14] and is proposed to trigger the transformation of MutL from an initiation mode to a processing mode.[16]

The presence of multiple DNA binding sites on Mlh1-Pms1 may be important for communication between the strand discrimination signal (e.g. possibly a nick or the primer termini at a replication fork) and proteins bound at the mismatch, such as Msh2-Msh6. For example, in the presence of ATP, binding of *E. coli* MutS protein to a mismatch results in formation of α-loop structures[12] that may be intermediates in the search for the strand discrimination signal. *E. coli* MutL enhances the yield of α-loops and it is found in a complex with MutS at the base of these structures where two dsDNA regions are juxtaposed. Perhaps MutL stabilizes this putative repair intermediate not only by interacting with MutS, but also by binding simultaneously to the two dsDNA regions that merge at the base of the α-loop. Other possible functions for multiple DNA binding sites exist as well. Two Mlh1-Pms1 binding sites for dsDNA may be relevant to repair on the leading and lagging strands during replication.

Current models of DNA mismatch repair also do not accommodate the present evidence for the cooperativity of DNA binding by Mlh1-Pms1 (Figures 3-6). In principle, cooperative interactions with duplex DNA could facilitate communication between the strand discrimination signal and the mismatch. Alternatively, physical interactions of Mlh1 and Pms1 with other components of the mismatch repair machinery may prevent cooperative assembly of Mlh1-Pms1 on DNA during mismatch repair. Cooperative interactions between Mlh1-Pms1 heterodimers, and DNA binding in general, may be relevant to the other DNA transactions in which these MutL homologs participate. These processes include meiotic recombination, transcription-coupled excision repair of DNA adducts, and other cellular responses to agents that damage DNA (for reviews on biological roles of mismatch repair proteins, see Buermeyer *et al*. and Harfe & Jinks-Robertson[1,3]).

The possible role of DNA binding by Mlh1-Pms1 in genetic recombination is of particular interest. Recombination involves homologous pairing of two DNA molecules over relatively long stretches. The cooperative, multiple-site DNA binding activity of Mlh1-Pms1 could be relevant here, although the two duplexes with which Mlh1-Pms1 simultaneously interacts (Figures 5 and 6) need not be homologous. It is clear from studies in mice that the MLH1 and PMS2 proteins are required for normal meiosis. Male mice deficient in PMS2 are sterile with spermatocytes exhibiting defective chromosome synapsis.[18] Male and female mice deficient in MLH1 are sterile and although chromosome synapsis is more or less normal, meiosis is arrested prematurely due to decreased crossing-over.[19,20] Moreover, MLH1 immunolocalizes to sites of crossing over in wild-type spermatocytes. In yeast, Mlh1 is also required for normal crossing over during meiosis.[21] It is currently unclear exactly how the MutL homologs act in meiosis to facilitate proper chromosome synapsis and crossing over. They could serve as part of the physical linkage between homologous chromosome pairs or at chiasmata. However, MLH1 and PMS2 may not even act together during meiosis, since the mice results show defects at different stages of meiosis depending on which gene is deficient. Also, it appears in yeast that Pms1 (homolog of mammalian PMS2) is not involved in meiotic crossing over.[21] Understanding the role of DNA binding by MutL homologs in recombination promises to be an exciting area of future research.

It will be interesting to determine if other dimeric MutL complexes possess a similar high affinity cooperative DNA binding activity. This may improve our understanding of the biological function of this DNA binding property. For example, if *E. coli* MutL protein binds cooperatively, then cooperative DNA binding would likely be relevant for biological processes common to prokaryotes and eukaryotes, such as mismatch repair, transcription-coupled nucleotide excision repair or prevention of homeologous recombination. In eukaryotes there are multiple dimeric MutL homolog complexes such as Mlh1-Mlh2 and Mlh1-Mlh3 in yeast and MLH1-PMS1 and MLH1-MLH3 in mammals. The different roles of these multiple complexes are only beginning to be understood. Studies of the DNA binding properties of these other heterodimers may also help provide further insight into their biological roles.

Materials and Methods

Overproduction and purification of Mlh1-Pms1

The procedure for overproduction and purification of Mlh1-Pms1 is described in detail elsewhere.[22] Protein concentrations were determined by the method of Bradford[35] using dye solution from Bio-Rad and bovine serum albumin (BSA) as a standard.

Materials

Strain SØ103 (*relA1 thyA144 rpsL254*(Str^r) *metB1 deoC4*)[36] was obtained from the *E. coli* Genetic Stock Center (Yale University, New Haven, CT). Strain SØ103 F′ was created by mating SØ103 with XL1-Blue (*recA1 endA1 gyrA96 thi-1 hsdR17 supE44 relA1 lac* [F′ *proAB lacI^{q}ZΔM15* Tn*10* (Tet^r)])(Stratagene) and selecting transconjugants on LB agar plates containing 25 μg/ml streptomycin and 10 μg/ml tetracycline. Media for growth of SØ103 F′ contained M9 minimal media salts, 12 mM glucose, 1 mM $MgSO_4$, 2.7 g/l salt-free casamino acids,

20 μM thymidine, and 25 μg/ml streptomycin. SØ103 carries *thyA* and *deoC* mutations that allow growth in media containing a very low thymidine concentration. This maximizes specific activity when labeling DNA *in vivo* with [^{3}H]thymidine. Phage T4 polynucleotide kinase, calf intestinal phosphatase, T4 DNA ligase, and all restriction enzymes were from New England Biolabs and were used under recommended conditions. DNase I (amplification grade) was from Life Technologies. 6-[^{3}H]thymidine and [γ-^{32}P]ATP were from Amersham Pharmacia Biotech. Poly(dA) was purchased from Sigma and the 100mer ssDNA oligonucleotide was synthesized by Life Technologies.

Preparation of DNA substrates

To prepare [^{3}H]M13mp2 phage DNA, a 10 ml overnight culture of SØ103 F′ was grown at 37 °C in minimal media described above. The overnight culture was diluted in 500 ml minimal media and grown for one hour at 37 °C prior to addition of 5×10^9 pfu of purified M13mp2 phage and 5 mCi [^{3}H]thymidine. Growth was continued for another nine hours at 37 °C. Phage particles were harvested and phage DNA purified as described.[37] The specific activity was 150,000 cpm/μg. To prepare [^{3}H]pGBT9 plasmid DNA, pGBT9 was transformed into SØ103 and a single transformant was grown at 37 °C up to one liter in minimal media supplemented with 150 μg/ml ampicillin and 4 mCi of [^{3}H]thymidine. Growth was continued overnight to saturation at 37 °C, cells were harvested by centrifugation and plasmid DNA purified using a QIAgen mega prep kit followed by a CsCl/EtBr gradient. The specific activity was 92,000 cpm/μg. Nicked circular [^{3}H]pGBT9 was generated by treating 9 μg of supercoiled DNA with 0.01 unit of DNase I for five minutes at room temperature. The reaction was quenched by adding EDTA to 2.5 mM and incubating at 65 °C for 20 minutes. Linear [^{3}H]pGBT9 was generated by digestion of approximately 25 μg supercoiled DNA with 20 units *Pst*I restriction endonuclease at 37 °C overnight followed by purification from a 0.8 % (w/v) agarose gel using the QIAquick gel extraction kit (QIAgen).

Poly(dA) and the 100mer oligonucleotide were 5′ end-labeled with ^{32}P by reaction with T4 polynucleotide kinase and [γ-^{32}P]ATP at 37 °C for one hour. The 100mer oligonucleotide was separated from unincorporated nucleotide using a QIAquick nucleotide removal kit (QIAgen). Poly(dA) was separated from unincorporated nucleotide on an STE-equilibrated Bio-Gel A-15 m column. The specific activities (cpm/μg) were 1.4×10^9 and 4.8×10^7 for the 100mer and poly(dA), respectively. The series of variable length linear duplex DNA molecules was generated by digestion of 68 μg of unlabeled pGBT9 plasmid DNA with ten units of *Bsr*BI, five units *Fsp*I, ten units *Hin*cII, or ten units *Acc*I overnight at 37 °C. Restriction reaction products were separated on a 1 % (w/v) TAE-agarose gel run in the presence of 0.5 μg/ml EtBr and the 3482 bp, 1801 bp and 241 bp *Bsr*BI fragments, the 1054 bp and 513 bp *Fsp*I fragments, the 5339 bp and 153 bp *Hin*cII fragments and the 84 bp *Acc*I fragment were purified using the QIAquick gel extraction kit (QIAgen). Each fragment was treated with calf intestinal phosphatase at 37 °C for one hour, 5′ end-labeled with T4 polynucleotide kinase and [γ-^{32}P]ATP at 37 °C for one hour and separated from unincorporated nucleotide using the QIAquick nucleotide removal kit. The concentration of each substrate was measured by absorption at 260 nm and adjusted to 10 μM DNA nucleotide. Specific activities (cpm/μg) were: 84 bp, 2.2×10^7; 153 bp, 1.5×10^7; 241 bp, 6.6×10^6; 513 bp, 4.1×10^6; 1054 bp, 1.9×10^6; 1801 bp, 1.5×10^6; 3482 bp, 9.6×10^5; 5339 bp, 7.1×10^5. ^{32}P-labeled Holliday junction and Y-junction substrates with arms of ~27 bp were donated by Dr Anna Fabisiewicz and Dr Leroy Worth (NIEHS).

To construct the 1.8 kb plasmid pMH10, pET3c (Novagen) was digested with *Bsr*BI. The resulting 1.8 kb fragment containing the origin of replication and the gene encoding β-lactamase was gel-purified, religated with T4 DNA ligase and recovered in *E. coli* XL1-Blue.

Nitrocellulose filter binding

Nitrocellulose filters (25 mm, 0.45 μm, HAWP, Millipore Corporation) were soaked in 0.4 M KOH for 20 minutes, rinsed thoroughly with deionized distilled water and soaked in binding buffer (25 mM Tris-HCl (pH 8.0), 10 % glycerol, 25 mM NaCl, 4 mM $MgCl_2$, 1 mM DTT) for at least one hour prior to use. Unless otherwise stated, binding reactions (20 μl) were performed in binding buffer supplemented with 100 μg/ml BSA. These binding conditions were selected based on the results presented in Figure 1. It should be noted that binding reactions were performed in the presence of $MgCl_2$ for consistency with atomic force microscopy experiments (see below), which require magnesium for deposition of DNA on the negatively charged mica surface. DNA substrate and Mlh1-Pms1 were included at the indicated concentrations. All binding reactions were incubated at room temperature (23-25 °C) for either five or ten minutes. It was empirically determined that binding was completed in less than 30 seconds and varying the length of incubation did not influence results. Following incubation, binding reactions were diluted with 1 ml of binding buffer and passed through nitrocellulose filters at a flow rate of approximately 2 ml/minute using a Millipore 1225 sampling vacuum manifold. Filters were rinsed once with 750 μl of binding buffer, dried under a heat lamp and quantitated with a Beckman LS 7800 liquid scintillation counter and EcoLume scintillation fluid (ICN). Background counts were measured in mock reactions lacking protein and although they varied somewhat depending on the DNA substrate, were typically less than 1 % of the total radioactivity.

Atomic force microscopy

Binding reaction mixtures (20 μl) contained 35 nM Mlh1-Pms1 and either 15 μM pMH10 or 8.7 μM M13mp2 dsDNA (nucleotide concentration) in binding buffer. Reactions were incubated at room temperature for one minute, then deposited on freshly cleaved ruby mica (Spruce Pine Mica Company, Spruce Pine, NC). Following an additional one minute incubation, excess liquid was blotted with Whatman filter paper and the mica was rinsed thoroughly with Nanopure water and dried under a nitrogen gas flow. All images were obtained with a Nanoscope III (Digital Instruments, Santa Barbara, CA) operated in tapping mode in air. Non-contact/tapping mode Nanosensor Pointprobe^R silicon cantilevers (Molecular Imaging Corporation) with force constants from 37.0 to 50.0 N/m were used for all imaging. The typical resonant frequency of these tips was approximately 180 kHz. The images were collected at 2.5-3.0 kHz scan speed and 512 × 512 resolution. Section analysis was performed using the Nanoscope software (version 4.42r4).

Acknowledgments

We thank Steve Matson and Leroy Worth for critical comments on the manuscript. This work was supported in part by National Institutes of Health grant ES09895 to D.E.

References

1. Buermeyer, A. B., Deschenes, S. M., Baker, S. M. & Liskay, R. M. (1999). Mammalian DNA mismatch repair. *Annu. Rev. Genet.* **33**, 533-564.
2. Kolodner, R. D. & Marsischky, G. T. (1999). Eukaryotic DNA mismatch repair. *Curr. Opin. Genet. Dev.* **9**, 89-96.
3. Harfe, B. D. & Jinks-Robertson, S. (2000). DNA mismatch repair and genetic instability. *Annu. Rev. Genet.* **34**, 359-399.
4. Lahue, R. S., Au, K. G. & Modrich, P. (1989). DNA mismatch correction in a defined system. *Science,* **245**, 160-164.
5. Su, S.-S. & Modrich, P. (1986). *Escherichia coli mutS*-encoded protein binds to mismatched DNA base-pairs. *Proc. Natl Acad. Sci. USA,* **83**, 5057-5061.
6. Grilley, M., Welsh, K. M., Su, S.-S. & Modrich, P. (1989). Isolation and characterization of the *Escherichia coli mutL* gene product. *J. Biol. Chem.* **264**, 1000-1004.
7. Au, K. G., Welsh, K. M. & Modrich, P. (1992). Initiation of methyl-directed mismatch repair. *J. Biol. Chem.* **267**, 12142-12148.
8. Ban, C. & Yang, W. (1998). Crystal structure and ATPase activity of MutL: implications for DNA repair and mutagenesis. *Cell,* **95**, 541-552.
9. Hall, M. C. & Matson, S. W. (1999). The *Escherichia coli* MutL protein physically interacts with MutH and stimulates the MutH-associated endonuclease activity. *J. Biol. Chem.* **274**, 1306-1312.
10. Grilley, M., Griffith, J. & Modrich, P. (1993). Bidirectional excision in methyl-directed mismatch repair. *J. Biol. Chem.* **268**, 11830-11837.
11. Hall, M. C., Jordan, J. R. & Matson, S. W. (1998). Evidence for a physical interaction between the *Escherichia coli* methyl-directed mismatch repair proteins MutL and UvrD. *EMBO J.* **17**, 1535-1541.
12. Allen, D. J., Makhov, A., Grilley, M., Taylor, J., Thresher, R., Modrich, P. & Griffith, J. D. (1997). MutS mediates heteroduplex loop formation by a translocation mechanism. *EMBO J.* **16**, 4467-4476.
13. Yamaguchi, M., Dao, V. & Modrich, P. (1998). MutS and MutL activate helicase II in a mismatch-dependent manner. *J. Biol. Chem.* **273**, 9197-9201.
14. Spampinato, C. & Modrich, P. (2000). The MutL ATPase is required for mismatch repair. *J. Biol. Chem.* **275**, 9863-9869.
15. Bende, S. M. & Grafstrom, R. H. (1991). The DNA binding properties of the MutL protein isolated from *Escherichia coli*. *Nucl. Acids Res.* **19**, 1549-1555.
16. Ban, C., Junop, M. & Yang, W. (1999). Transformation of MutL by ATP binding and hydrolysis: a switch in DNA mismatch repair. *Cell,* **97**, 85-97.
17. Mechanic, L. E., Frankel, B. A. & Matson, S. W. (2000). *Escherichia coli* MutL loads DNA helicase II onto DNA. *J. Biol. Chem.* **275**, 38337-38346.
18. Baker, S. M., Bronner, C. E., Zhang, L., Plug, A. W., Robatzek, M. & Warren, G. *et al*. (1995). Male mice defective in the DNA mismatch repair gene *PMS2* exhibit abnormal chromosome synapsis in meiosis. *Cell,* **82**, 309-319.
19. Baker, S. M., Plug, A. W., Prolla, T. A., Bronner, C. E., Harris, A. C. & Yao, X. *et al*. (1996). Involvement of mouse *Mlh1* in DNA mismatch repair and meiotic crossing over. *Nature Genet.* **13**, 336-342.
20. Edelmann, W., Cohen, P. E., Kane, M., Lau, K., Morrow, B. & Bennett, S. *et al*. (1996). Meiotic pachytene arrest in MLH1-deficient mice. *Cell,* **85**, 1125-1134.
21. Hunter, N. & Borts, R. H. (1997). Mlh1 is unique among mismatch repair proteins in its ability to promote crossing-over during meiosis. *Genes Dev.* **11**, 1573-1582.
22. Hall, M. C. & Kunkel, T. A. (2001). Purification of eukaryotic MutL homologs from *Saccharomyces cerevisiae* using self-cleaving affinity technology. *Protein Exp. Purif.* **21**, 333-342.
23. Record, M. T., Jr, deHaseth, P. L. & Lohman, T. M. (1977). Interpretation of monovalent and divalent cation effects on the *lac* repressor-operator interaction. *Biochemistry,* **16**, 4791-4796.
24. Habraken, Y., Sung, P., Prakash, L. & Prakash, S. (1997). Enhancement of MSH2-MSH3-mediated mismatch recognition by the yeast MLH1-PMS1 complex. *Curr. Biol.* **7**, 790-793.
25. Habraken, Y., Sung, P., Prakash, L. & Prakash, S. (1998). ATP-dependent assembly of a ternary complex consisting of a DNA mismatch and the yeast MSH2-MSH6 and MLH1-PMS1 protein complexes. *J. Biol. Chem.* **273**, 9837-9841.
26. Gradia, S., Subramanian, D., Wilson, T., Acharya, S., Makhov, A., Griffith, J. & Fishel, R. (1999). hMSH2-hMSH6 forms a hydrolysis-independent sliding clamp on mismatched DNA. *Mol. Cell.* **3**, 255-61.
27. Lamers, M. H., Perrakis, A., Enzlin, J. H., Winterwerp, H. H. K., de Wind, N. & Sixma, T. K. (2000). The crystal structure of DNA mismatch repair protein MutS binding to a G-T mismatch. *Nature,* **407**, 711-717.
28. Obmolova, G., Ban, C., Hsieh, P. & Yang, W. (2000). Crystal structures of mismatch repair protein MutS and its complex with a substrate DNA. *Nature,* **407**, 703-710.
29. Hansma, H. G., Laney, D. E., Bezanilla, M., Sinsheirmer, R. & Hansma, P. K. (1995). Applications for atomic force microscopy of DNA. *Biophys. J.* **68**, 1672-1677.
30. Keller, D. J. (1991). Reconstruction of STM and AFM images distorted by finite size tips. *Surf. Sci.* **253**, 353-364.
31. Fritz, M., Radmacher, M., Clevelend, J. P., Allersma, M. W., Stewart, R. J. & Gieselman, R. *et al*. (1995). Imaging globular and filamentous proteins in physiological buffer solutions with tapping mode atomic force microscopy. *Langmuir,* **11**, 3529-3535.
32. Hansma, H. G., Revenko, I., Kim, K. & Laney, D. E. (1996). Atomic force microscopy of long and short double-stranded, single-stranded and triple-stranded nucleic acids. *Nucl. Acids Res.* **24**, 713-720.
33. Menetski, J. P. & Kowalczykowski, S. C. (1987). Transfer of recA protein from one polynucleotide to another. *J. Biol. Chem.* **262**, 2085-2092.
34. Jiricny, J. (1998). Eukaryotic mismatch repair: an update. *Mutat. Res.* **409**, 107-121.

35. Bradford, M. M. (1976). A rapid and sensitive method for the quantitation of microgram quantities of protein utilizing the principle of protein-dye binding. *Anal. Biochem.* **72**, 248-254.
36. Munch-Petersen, A., Nygaard, P., Hammer-Jespersen, K. & Fiil, N. (1972). Mutants constitutive for nucleoside-catabolizing enzymes in *Escherichia coli* K12. Isolation, characterization and mapping. *Eur. J. Biochem.* **27**, 208-215.
37. Bebenek, K. & Kunkel, T. A. (1995). Analyzing fidelity of DNA polymerases. *Methods Enzymol.* **262**, 217-232.

Edited by M. Belfort

(Received 2 April 2001; received in revised form 19 July 2001; accepted 25 July 2001)

http://www.academicpress.com/jmb

Supplementary Material for this paper is available on IDEAL